

# Comparison of activation of aristolochic acid I and II with NADPH:quinone oxidoreductase, sulphotransferases and *N*-acetyltransferases

Vaclav MARTINEK<sup>1</sup>, Bozena KUBICKOVA<sup>1</sup>, Volker M ARLT<sup>2</sup>, Eva FREI<sup>3</sup>, Heinz H SCHMEISER<sup>4</sup>, Jiri HUDECEK<sup>1</sup>, Marie STIBOROVA<sup>1</sup>

<sup>1</sup> Department of Biochemistry, Faculty of Science, Charles University, Prague, Czech Republic

<sup>2</sup> Section of Molecular Carcinogenesis, Institute of Cancer Research, Brookes Lawley Building, Sutton, Surrey, UK

<sup>3</sup> Division of Preventive Oncology, National Center for Tumour Diseases, German Cancer Research Center, Heidelberg, Germany

<sup>4</sup> Research Group Genetic Alterations in Carcinogenesis, German Cancer Research Center, Heidelberg, Germany

*Correspondence to:* Prof. RNDr. Marie Stiborova, DSc.  
Department of Biochemistry, Faculty of Science, Charles University  
Albertov 2030, 128 40 Prague 2, Czech Republic.  
TEL: +420-221 951; FAX: +420-221 951 283; E-MAIL: stiborov@natur.cuni.cz

*Submitted:* 2011-05-20 *Accepted:* 2011-08-25 *Published online:* 2011-11-05

*Key words:* aristolochic acid; NAD(P)H:quinone oxidoreductase; sulfotransferase; acetyltransferase; DNA adducts; molecular modeling

Neuroendocrinol Lett 2011;32(Suppl.1):57-70 PMID: 22167209 NEL32S111A07 © 2011 Neuroendocrinology Letters • www.nel.edu

## Abstract

**OBJECTIVES:** Ingestion of aristolochic acid (AA) is associated with development of urothelial tumors linked with aristolochic acid nephropathy, and is implicated in the development of Balkan endemic nephropathy-associated urothelial tumors. Aristolochic acid I (AAI), the major toxic component of AA, is more toxic than its demethoxylated derivate AAI. A different enzymatic conversion of both carcinogens might be one of the reasons explaining this feature. Therefore, the present study has been designed to compare efficiency of human NAD(P)H:quinone oxidoreductase (NQO1) and phase II enzymes such as sulfotransferases (SULTs) and *N,O*-acetyltransferases (NATs) to activate AAI and AAI *in vitro*. In addition, to investigate the molecular mechanisms of AAI and AAI reduction by human NQO1, molecular modeling was used to compare interactions of AAI and AAI with the active site of this enzyme.

**METHODS:** DNA adduct formation by AAI and AAI was investigated by the nuclease P1 version of the <sup>32</sup>P-postlabeling method. *In silico* docking, employing soft-soft (flexible) docking procedure, was used to study the interactions of AAI and AAI with the active site of human NQO1.

**RESULTS:** Human NQO1 activated AAI and AAI, generating DNA adduct patterns reproducing those found in several species including human exposed to these compounds. These results demonstrate that NQO1 is capable of reducing both AAs to reactive species binding to DNA. However, concentrations required for half-maximum DNA binding mediated by NQO1 were higher for AAI (158 μM) than for AAI (17 μM). One of the reasons causing this phenomenon is a lower efficiency of NQO1 to reduce AAI than AAI we found in this work; although both AAI and AAI are bound with similar binding affinities to the NQO1 active site, the binding orientation of AAI in the active site of NQO1 does not favor

the effective reduction of its nitro group. Because reduced nitro-aromatics are often further activated by SULTs or NATs, their roles in AAI and AAI activation were investigated. Our results indicate that phase II reactions do not stimulate the bioactivation of AAs; neither enzymes present in human hepatic cytosols nor human SULT1A1, 1A2, 1A3, 1E, or 2A nor NAT1 or NAT2 further enhanced DNA adduct formation by AAs. In contrast, human SULT1A1, 1A2 and 1A3 as well as NAT1 and NAT2 enzymes even inhibited NQO1-mediated bioactivation of AAI. Therefore, under the *in vitro* conditions used, DNA adducts arise by enzymatic reduction of AAs through the formation of *N*-hydroxyaristolactams that are spontaneously decomposed to the reactive species forming DNA adducts.

**CONCLUSION:** The results found in this study emphasize the importance of NQO1 in the metabolic activation of AAI and AAI and provide the evidence that initial nitroreduction is the rate limiting step in their activation. This enzyme is more effective in activation of AAI relative to AAI, which might contribute to its lower binding to DNA found both *in vitro* and *in vivo*. Moreover, inhibition effects of conjugation reactions on AAI activation might further contribute to its decreased capability of forming DNA adducts and its lower toxicity comparing with AAI.

#### Abbreviations:

AA	- aristolochic acid
AAI	- 8-methoxy-6-nitro-phenanthro-(3,4- <i>d</i> )-1,3-dioxolo-5-carboxylic acid
AAII	- 6-nitro-phenanthro-(3,4- <i>d</i> )-1,3-dioxolo-5-carboxylic acid
CYP	- cytochrome P450
dA-AAI	- 7-(deoxyadenosin- <i>N</i> <sup>6</sup> -yl)aristolactam I
dA-AAII	- 7-(deoxyadenosin- <i>N</i> <sup>6</sup> -yl)aristolactam II
dG-AAI	- 7-(deoxyguanosin- <i>N</i> <sup>2</sup> -yl) aristolactam I
HPLC	- high performance liquid chromatography
NADPH	- nicotinamide adenine dinucleotide phosphate (reduced)
NQO1	- NAD(P)H:quinone oxidoreductase
PEI	- polyethylenimine
RAL	- relative adduct labeling
TLC	- thin layer chromatography
SULTS	- sulfotransferase
NAT	- <i>N,O</i> -acetyltransferase

## INTRODUCTION

The so-called Chinese herbs nephropathy (now termed aristolochic acid nephropathy (Arlt *et al.* 2002b; Debelle *et al.* 2008; Schmeiser *et al.* 2009) was observed for the first time in a group of Belgian women after ingestion of "slimming" pills containing *Aristolochia fangchi* (Vanherweghem *et al.* 1993). It is a rapidly progressive renal fibrosis; the patients developed subsequently a high risk of upper urothelial tract carcinoma (about 50%) and bladder urothelial carcinoma (Nortier *et al.* 2000; Lemy *et al.* 2008). This nephropathy has been shown to be caused by the aristolochic acid (AA) derived from Aris-

tolochia species. Later, similar cases have been reported elsewhere in Europe and Asia (Lord *et al.* 2001; Debelle *et al.* 2008; Lai *et al.* 2010). In addition, this compound has been linked also to another nephropathy, the Balkan endemic nephropathy and its associated urothelial cancer (Arlt *et al.* 2007; Grollman *et al.* 2007; Nedelko *et al.* 2009). Balkan endemic nephropathy is endemic in certain rural areas of Serbia, Bosnia, Croatia, Bulgaria and Romania. In urothelial tissue of patients suffering from both nephropathies, specific AA-DNA adducts were identified (Schmeiser *et al.* 1996; Bieler *et al.* 1997; Nortier *et al.* 2000; Lord *et al.* 2001; Arlt *et al.* 2002a; Grollman *et al.* 2007)..

The AA, as extracted from plants of *Aristolochiaceae* family, is a mixture of structurally related nitrophenanthrene carboxylic acids, with two major components (see Figure 1), AAI (8-methoxy-6-nitro-phenanthro-(3,4-*d*)-1,3-dioxolo-5-carboxylic acid, AAI) and AAI (6-nitro-phenanthro-(3,4-*d*)-1,3-dioxolo-5-carboxylic acid, AAI). Both compounds are mutagenic and genotoxic (Schmeiser *et al.* 1984; Arlt *et al.* 2002b; Kohara *et al.* 2002; Mei *et al.* 2006), forming covalent adducts with DNA (Figure 1) (Schmeiser *et al.* 1988). Metabolic activation proceeds *via* partial reduction of the nitro group, forming cyclic *N*-acylnitrenium ion with a delocalized positive charge (aristolactam-nitrenium ion) is the ultimate electrophilic species (Figure 1). Both nitroso and *N*-hydroxy derivatives, formed by reduction of the nitro group, are stabilized by *peri* interaction. Condensation of an *N*-hydroxyl group with the carboxylic acid moiety in *peri* position leads to a cyclic hydroxamic acid (*N*-hydroxyaristolactam), which has been identified recently in the urine of AA-treated rats (Chan *et al.* 2007). This is a likely precursor of the pentacyclic nitrenium ion, which can be converted to an isomeric carbonium ion able to bind covalently to DNA *via* the C7 position. Among the major DNA-adducts found in rodents and humans exposed to AA are 7-(deoxyadenosin-*N*<sup>6</sup>-yl)aristolactam I (dA-AAI), 7-(deoxyadenosin-*N*<sup>6</sup>-yl)aristolactam II (dA-AAII), 7-(deoxyguanosin-*N*<sup>2</sup>-yl)aristolactam I (dG-AAI) and 7-(deoxyguanosin-*N*<sup>2</sup>-yl) aristolactam II (dG-AAII). On the other hand, the prevailing adduct detected in patients exposed to AA is 7-(deoxyadenosin-*N*<sup>6</sup>-yl)-aristolactam I (dA-AAI) (Figure 1), which causes characteristic AT→TA transversion mutations. Such AT→TA mutations have been reported in the *TP53* tumor suppressor gene in tumors from patients suffering from Balkan and aristolochic acid nephropathies (Lord *et al.* 2004; Arlt *et al.* 2007; Grollman *et al.* 2007; Nedelko *et al.* 2009). This indicates the probable molecular mechanism of AA carcinogenesis in humans (Simoes *et al.* 2008; Arlt *et al.* 2011), and justifies the recent classification of AA as carcinogenic to humans (Group 1) by the International Agency for Research on Cancer (Grosse *et al.* 2009).

Comparing the AAI to AAI, a significantly higher level of DNA binding of AAI was found in rats and mice

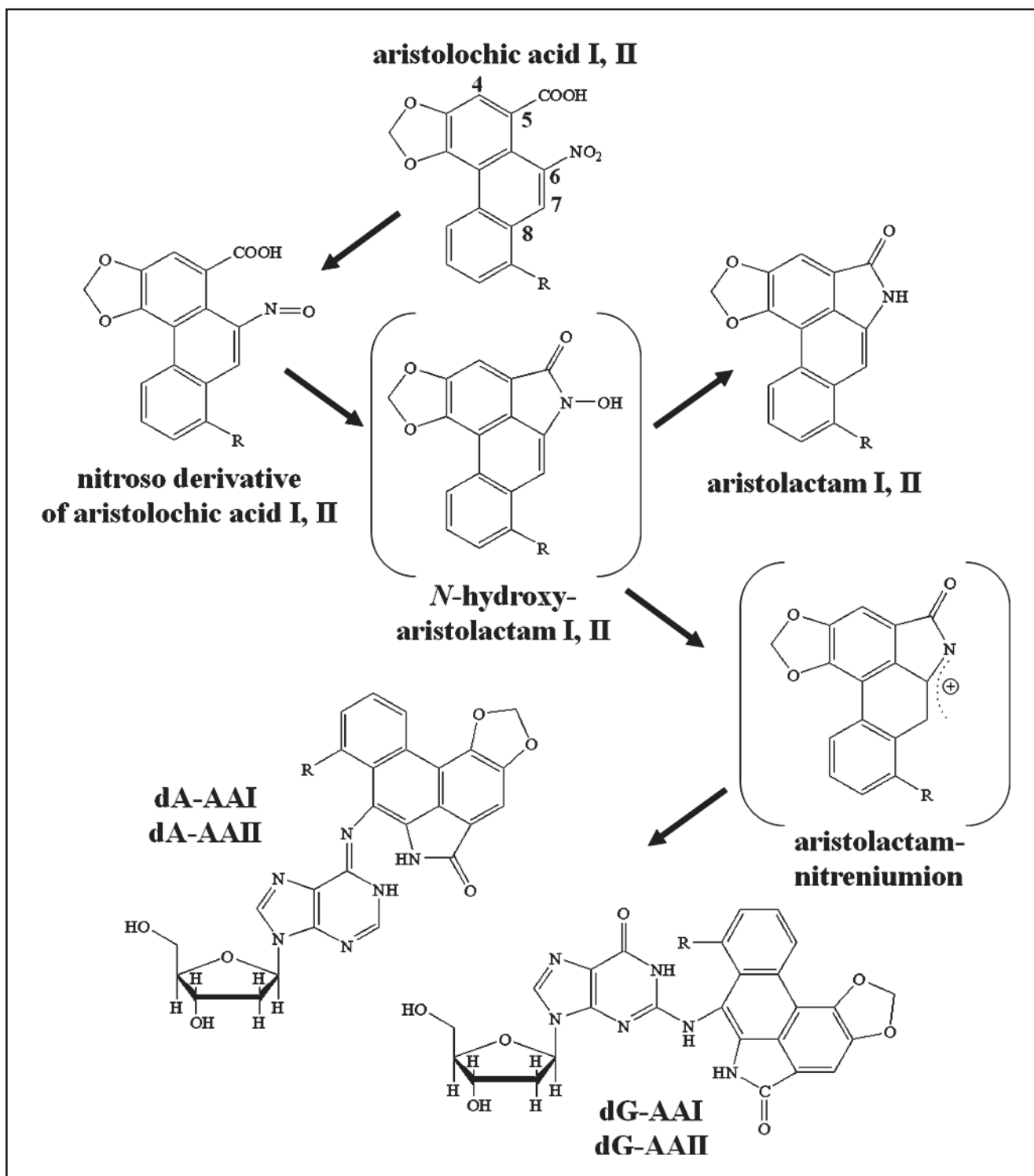


**Fig. 1.** Metabolic activation and DNA adduct formation of aristolochic acid I [8-methoxy-6-nitro-phenanthro-(3,4-d)-1,3-dioxolo-5-carboxylic acid, AAI; R = OCH<sub>3</sub>] and II [6-nitro-phenanthro-(3,4-d)-1,3-dioxolo-5-carboxylic acid, AAI; R = H]; 7-(deoxyadenosin-N<sup>6</sup>-yl) aristolactam I or II (dA-AAI or dA-AAII), 7-(deoxyguanosin-N<sup>2</sup>-yl)aristolactam I or II (dG-AAI or dG-AAII).

*in vivo* (Schmeiser *et al.* 1988; Pfau *et al.* 1990; Stiborova *et al.* 1994; Shibutani *et al.* 2007) and in several enzymatic systems *in vitro* (Schmeiser *et al.* 1997; Stiborova *et al.* 2001a; 2001b; 2001c; 2002). This difference might be explained by a different enzymatic conversion

of both carcinogens, with AAI being probably poorer substrate of the reduction-catalyzing enzymes.

Similarly to other nitroaromatics, the nitroreduction is the major activation pathway for both AAI and AAI. This reaction can be catalyzed by both cytosolic

and microsomal enzymes, as the most efficient one, the cytosolic NAD(P)H:quinone oxidoreductase (NQO1) has been shown (Stiborova *et al.* 2002; 2003; 2008a; 2008b; 2011) (Figure 1). In human hepatic microsomes, the activation of both AAs is mediated mainly by cytochrome P450 (CYP1) A2. A minor role is played also by CYP1A1 and NADPH:CYP reductase (Stiborova *et al.* 2001b; 2001c; 2005a; 2005b; 2008a; 2008b); also prostaglandin H synthase (cyclooxygenase) has been shown to activate both AAs in human renal microsomes (Stiborova *et al.* 2001a; 2005a)

The conjugation reactions catalyzed by phase II enzymes are known to be important in the metabolic activation of carcinogenic nitroaromatics and aromatic amines (for review see Glatt 2000; Glatt *et al.* 2001; Hein 2002; Hein *et al.* 2000). The *N*-hydroxyaristolactam may be further activated by *O*-acetylation or *O*-sulfonation to unstable esters capable of forming nitrenium and carbenium ions faster than nitro reduction alone, as has been shown for other aromatic hydroxylamines (Arlt *et al.* 2005). However, our recent results indicate that phase II reactions seem not to play any major role in bioactivation of AAI (Stiborova *et al.* 2011).

The present study is focused on AAI and on a comparison of this compound to AAI with respect to reductive activation, species forming DNA adducts and also to the role of human sulfotransferases (SULTs) and *N,O*-acetyltransferases (NATs) in the process of activation of these carcinogens. To this end, a similar methodology as in our previous work (Stiborova *et al.* 2011) was used. We studied the influence of cofactors of SULTs and NATs on AAI- and AAI-derived DNA adduct formation generated *in vitro* in human cytosols. In addition to this, we used also human recombinant NQO1 in combination with individual recombinant NATs or SULTs.

## MATERIALS AND METHODS

### Chemicals

NADPH, acetyl coenzyme A (acetyl-CoA), 3'-phosphoadenosine-5'-phosphosulfate, the natural mixture of AA consisting of 38% AAI and 58% AAI was purchased from Sigma Chemical Co (St Louis, MO, USA) and calf thymus DNA were from Sigma Chemical Co (St Louis, MO, USA). AAI and AAI were isolated from the mixture by preparative HPLC; their purity were ~99% as estimated by HPLC (Schmeiser *et al.* 1984; 1988). Male human hepatic cytosols were from Gentest Corp. (samples cat. no. H806 and H856; Woburn, MA, USA). Cytosol from one human kidney (specimen from European Transplant Centre was a gift from Dr. Joelle Nortier, Hôpital Erasme, Brussels, Belgium) was prepared by differential centrifugation (Stiborova *et al.* 2001d; 2003; Svobodova *et al.* 2009). The age, drug and alcohol history of the kidney donor are not known, but they are known for the liver donors. Cytosolic extracts, isolated from insect cells transfected with baculovirus

constructs containing human cDNA of SULT1A1\*2, 1A2\*1, 1A3, 1E or 2A1 were obtained from Oxford Biomedical Research Inc. (Oxford, MA, USA), and those containing cDNA of human NAT1\*4 or NAT2\*4 from Gentest (Woburn, MA, USA). Cytosolic extracts expressing SULT1A1 and SULT1A2 conjugated *p*-nitrophenol at rates of 124 and 5.5 nmol/min/mg protein, respectively; SULT1A3 conjugated dopamine at the rate of 8 nmol/min/mg protein; SULT1E conjugated estrone at the rate of 266 pmol/min/mg protein; and SULT2A1 conjugated dehydroepiandrosterone at the rate of 584 pmol/min/mg protein. Cytosolic extracts expressing NAT1 and NAT2 had a catalytic activity of 1300 nmol/min/mg protein (substrate *p*-aminosalicylic acid) and 290 nmol/min/mg protein (substrate sulfamethazine), respectively. Enzyme activities in control cytosol were less than 10 pmol/min/mg protein. Enzymes and chemicals for the <sup>32</sup>P-postlabeling assay were obtained from sources described (Stiborova *et al.* 2005a; Phillips & Arlt 2007). All these and other chemicals were reagent grade or better.

### Incubations

The deaerated and argon-purged incubation mixtures, (final volume 750 µl), were essentially 50 mM Tris-HCl buffer (pH 7.4), with 0.2% Tween 20, up to 0.5 mM AAI or AAI (as sodium salts dissolved in water), containing 0.5 mg of calf thymus DNA. To this "basic" incubation mixture, the "activating component" was added (see below). The reaction was initiated by adding NADPH to the final concentration of 1 mM. Incubations were carried out at 37°C. Control incubations were carried out (i) without "activating component", (ii) without NADPH, (iii) without DNA or (iv) without AA. 3-Nitrobenzanthrone was used as positive control (Arlt 2005; Arlt *et al.* 2005; Stiborova *et al.* 2010a). After incubation for the desired period of time, the mixture was extracted twice with ethyl acetate (2 x 2 ml), DNA was isolated from the residual water phase by the phenol/chloroform extraction method as described (Stiborova *et al.* 1988; 2003; 2005a; 2010b). The conditions for particular experiments were as follows: in cytosolic incubations 1 mg of human hepatic or renal cytosolic protein was added as the activating component, and the mixture incubated for 60 min; the cytosol-mediated AAI- and AAI-derived DNA adduct formation was found to be linear up to 2 hr (Stiborova *et al.* 2002; 2003). Assays for SULT- and NAT-dependent bioactivation in human cytosolic samples were carried out using either 1 or 2 mM acetyl-CoA or 0.2 or 0.4 mM 3'-phosphoadenosine-5'-phosphosulfate, which were added to the incubation mixtures described above, respectively, using procedures analogous to those reported previously (Arlt *et al.* 2005).

### Incubations with human recombinant NQO1

To the incubation mixture described above, containing 0.05–0.5 mM AAI or AAI, 0–20 µg (0–0.06 units)

of NQO1 were added. One unit of NQO1 is defined as that needed to reduce 1  $\mu\text{mol}$  of cytochrome *c* per min in the presence of menadione as substrate at 37°C.; NQO1-mediated AAI-derived DNA adduct formation was found to be linear up to 90 min (see text for detail). In control incubations NQO1 was omitted from the mixtures. In incubations using cytosols of baculovirus-transfected insect cells containing recombinant SULT1A1, 1A2, 1A3, 1E, 2A1, NAT1 or NAT2, an additional 50  $\mu\text{g}$  of the respective enzyme was added to the reaction mixture with NQO1. Cytosolic fractions isolated from insect cells, which were not transfected with any human transferases, were used as controls. After the incubation, DNA was isolated by the phenol/chloroform extraction method as described above.

Incubations for kinetic studies with human recombinant NQO1 were the same as those described above except that they contained 0–0.5 mM AAI or AAI, 0–20  $\mu\text{g}$  human recombinant NQO1 and incubation times varied between 0 and 100 min. Kinetic analyses were carried out using the non-linear least-squares method described by Cleland (1983).

#### DNA adduct analysis by $^{32}\text{P}$ -postlabeling

$^{32}\text{P}$ -Postlabeling analysis (Phillips & Arlt 2007) using the nuclease P1 enrichment version, and thin layer chromatography (TLC), and HPLC were performed as described (Stiborova *et al.* 1994; 2010b; Bieler *et al.* 1997; Schmeiser *et al.* 1997). Chromatographic conditions for TLC on polyethylenimine (PEI)-cellulose plates (10 cm  $\times$  20 cm; Macherey-Nagel, Düren, Germany) were: D1, 1.0 M sodium phosphate, pH 6.8; D3: 3.5 lithium-formate, 8.5 M urea, pH 4; D4, 0.8 M lithium chloride, 0.5 M Tris-HCl, 8.5 M urea, pH 9; D5, 1.7 M sodium phosphate, pH 6. After chromatography TLC sheets were scanned using a Packard Instant Imager (Dowers Grove, USA) and DNA adduct levels (RAL, relative adduct labeling) were calculated as described (Stiborova *et al.* 1994; 2010b; Bieler *et al.* 1997; Schmeiser *et al.* 1997). AA-DNA adducts were identified using reference compounds as described (Stiborova *et al.* 1994).

#### Molecular docking of AAI, AAI, their nitroso-derivatives and N-hydroxyaristolactams into NQO1

The procedure was described in detail in our previous work (Stiborova *et al.* 2011). Briefly, the 3D model of the human NQO1 enzyme was based on crystal structure (2.50 Å resolution; PDB ID 1DXO) (Faig *et al.* 2000) containing a small planar ligand (duroquinone), stacking with the isoalloxazine ring of FAD. This crystal structure contains cofactors in their oxidized state. We examined the affinity of all substrates to the enzyme in the reduced state, therefore reduced FAD was used in the flexible docking procedure. Only an anionic form (deprotonated at N1) or the protonated enol form with hydrogens on N5 and O2 of the isoalloxazine ring of FAD are considered to be present in the active site of

NQO1 (Li *et al.* 1995; Cavelier & Amzel 2001; Stiborova *et al.* 2010a; 2011), both were used here.

The modeled system used for docking calculation consisted of biologically active NQO1 as a homodimeric protein complex (Ross *et al.* 2000; Faig *et al.* 2001) of two tightly interacting monomers (273 residues each) with two active sites. During structure preparation, hydrogen atoms were added and crystallographic water and the duroquinone ligand molecules were removed, usual protonation states and partial charges were assigned to all residues (His residues were protonated). The geometries and charges of ligands [AAI, AAI, their nitroso-derivatives (AAI-NO, AAI-NO) and N-hydroxyaristolactams] were obtained by *ab initio* calculations on the Hartree-Fock level of theory in conjunction with the 6-31+G(d) basis set. *Ab initio* calculations were performed with Gaussian03 (Frisch *et al.* 2003). We employed a hybrid global-local Lamarckian genetic algorithm implemented in modified AutoDock v4.2 program suite (Huey *et al.* 2007) to evaluate binding free energies and preferred binding modes for studied compounds. This version, more powerful than the version 3 used in our older work (Stiborova *et al.* 2003), combines two methods to find the most preferable binding modes, rapid grid-based energy evaluation and efficient search of torsional freedom, together with optional soft-soft docking. During the flexible docking procedure, both the position of the ligand and the orientations of the selected flexible side-chains are optimized simultaneously. In order to allow the enzyme to adapt a new ligand, we ran soft-soft docking calculations. All rotatable bonds of the ligands and four amino acid side chains, Tyr126 and Tyr128 (chain C in NQO1) and Trp105 and His161 (chain A in NQO1), were allowed to rotate freely. We performed an extensive search (2000 docking runs per compound) of the most preferred binding modes of AAI, AAI, their nitroso-derivatives and N-hydroxyaristolactam ligands within a 36  $\times$  48  $\times$  50 Å grid-box centered on the substrate binding cavity. Similar resulting structures (RMSD lower than 2.0 Å) were grouped and finally sorted by binding free energy of the best binding structure within each cluster. As a result, a number of binding modes with similar binding energies were obtained for every system, which was examined with focus on modes allowing an efficient reduction. Only an orientation with a sufficiently short distance between the N5 of the isoalloxazine ring and an oxygen atom of the nitro group would facilitate the hydride transfer preceding the nitro-reduction. Similarly, for the alternative three-step ( $e^-$ ,  $\text{H}^+$ ,  $e^-$ ) reduction mechanism, the discriminating distance was the separation of the OH group of Tyr128 and oxygen of the nitro-, nitroso- or N-hydroxyaristolactamoyl-group. Besides the binding free energy, this distance was used to evaluate the efficiency of the NQO1 catalyzed reduction of AAI, AAI, their nitroso-derivatives and N-hydroxyaristolactams.

## RESULTS

### Metabolic activation of AAI or AAI by human recombinant NQO1

Incubation of DNA with AAI or AAI (0.05–0.5 mM) with DNA, human recombinant NQO1 and its cofactor NADPH resulted in formation of DNA adducts. As shown in Figure 2, four major adducts 1,2,3 and 4 formed by AAs were detected using the nuclease P1 version of the  $^{32}\text{P}$ -postlabeling assay. Whereas the adduct pattern formed by AAI consisted of three major DNA adduct spots that were identified as 7-(deoxyguanosin- $\text{N}^2$ -yl)aristolactam I (spot 1; dG-AAI), 7-(deoxyadenosin- $\text{N}^6$ -yl)aristolactam I (spot 2; dA-AAI) and 7-(deoxyadenosin- $\text{N}^6$ -yl)aristolactam II (spot 3; dA-AAII) (Figure 2A), that by AAI consisted from two adduct spots, 7-(deoxyadenosin- $\text{N}^6$ -yl)-aristolactam II (dA-AAII, spot 3, dA-AAII) and 7-(deoxyguanosin- $\text{N}^2$ -yl)-aristolactam II (dG-AAII, spot 4) (Figure 2B). These

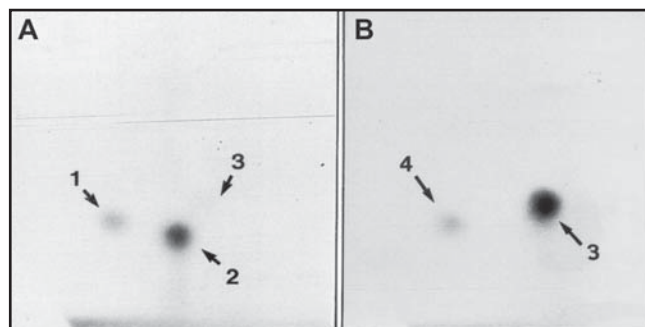


**Fig. 2.** Autoradiographic profiles of AAI-DNA (A) and AAI-DNA (B) adducts formed by incubation of AAI or AAI with human hepatic cytosol. The nuclease P1-enrichment procedure was used for analysis. Origins, in the bottom left-hand corner were cut off before exposure. Spot 1, dG-AAI; spot 2, dA-AAI; spot 3, dA-AAII; spot 4, dG-AAII.

adduct spots cochromatographed on PEI-cellulose TLC plates and by reversed-phase HPLC (not shown) with those of synthetic standards (Stiborova *et al.* 1994). AAI-DNA adducts generated by this enzymatic system were the same as those formed by human NQO1 found in our former studies (Stiborova *et al.* 2003; 2011) or by other activating systems (Stiborova *et al.* 2001a; 2001b; 2001c, 2002; 2003; 2005a; 2005b) and *in vivo* in rats and mice (Schmeiser *et al.* 1988; Pfau *et al.* 1990; Stiborova *et al.* 1994) or in humans (Schmeiser *et al.* 1996; Bieler *et al.* 1997; Nortier *et al.* 2000; Lord *et al.* 2001). Likewise, AAI-DNA adducts generated by human NQO1 were the same as those by other activating systems (Stiborova *et al.* 2001a; 2001b; 2001c,) and *in vivo* in rats (Schmeiser *et al.* 1988; Pfau *et al.* 1990; Stiborova *et al.* 1994). TLC autoradiograms of  $^{32}\text{P}$ -labeled DNA from control incubations carried out in parallel were devoid of adduct spots in the region of interest (data not shown).

The lowest concentration of AAI and AAI used (0.05 mM) induced a total DNA binding of 7.8 and 3.7 adducts/ $10^7$  nucleotides, respectively (Figure 3), with dA-AAI and dA-AAII being the most abundant adducts formed. However, at the highest concentrations of both AAs (0.5 mM), similar levels of total DNA adducts were detected ( $11.5 \pm 1.6$  and  $12 \pm 1.8$  adducts/ $10^7$  nucleotides for AAI and AAI, respectively, Figure 3). AAI- and AAI-DNA adduct levels mediated by NQO1 were dependent on the incubation time (being linear up to 90 min; Figure 3A and 3B), and on the AA (Figure 3C and 3D) and NQO1 concentration (Figure 3C and 3F). The concentration of AAI required for half-maximum DNA binding was  $158 \mu\text{M}$ , as extrapolated from double reciprocal plot of data (Figure 3D), in contrast to the value of  $17 \mu\text{M}$ , found previously for the AAI (Stiborova *et al.* 2011).

**Tab. 1.** The predicted binding free energies and distances facilitating the H-transfer for AAI, AAI and their reduced metabolites to human NQO1. Data for AAI and AAI-NO are taken from our previous work (Stiborova *et al.* 2011).

	NQO1 FADH $^-$ deprotonated (anionic form)		NQO1 enol-FADH $_2$ (protonated form)			
	direct H-transfer		direct H-transfer		mediated H-transfer (e $^-$ , H $^+$ , e $^-$ )	
	Estimated Free Energy of binding [kcal/mol]	N5(FAD)-O(AAI+der.) distance [Å] <sup>a</sup>	Estimated Free Energy of binding [kcal/mol]	N5(FAD)-O(AAI+der.) distance [Å] <sup>a</sup>	Estimated Free Energy of binding [kcal/mol]	OH(Y128)-O(AAI+der.) distance [Å] <sup>b</sup>
AAI	-6.4	3.2	-6.3	3.2	-7.9	2.8
AAI-NO	-5.4	3.6	-5.9	3.0	-7.6	2.8
AAI-N-hydroxy lactam	-5.3	4.6	-5.4	4.1	-6.1	2.9
AAII	-5.9	4.4	-6.5	4.4	-7.5	2.8
AAII-NO	-4.8	4.1	-5.2	3.3	-7.2	2.8
AAII- N-hydroxy lactam	-5.8	5.1	-5.9	5.0	-6.4	2.8

<sup>a</sup>Distance between the oxygen in nitro, nitroso or N-OH-lactamoyl group of AAI/II or their metabolites and nitrogen 5 of reduced FAD, see Fig. 4;

<sup>b</sup>Distance between the oxygen in nitro, nitroso or N-OH-lactamoyl group of AAI/II or their metabolites and OH group of Tyr128, see Fig. 5.

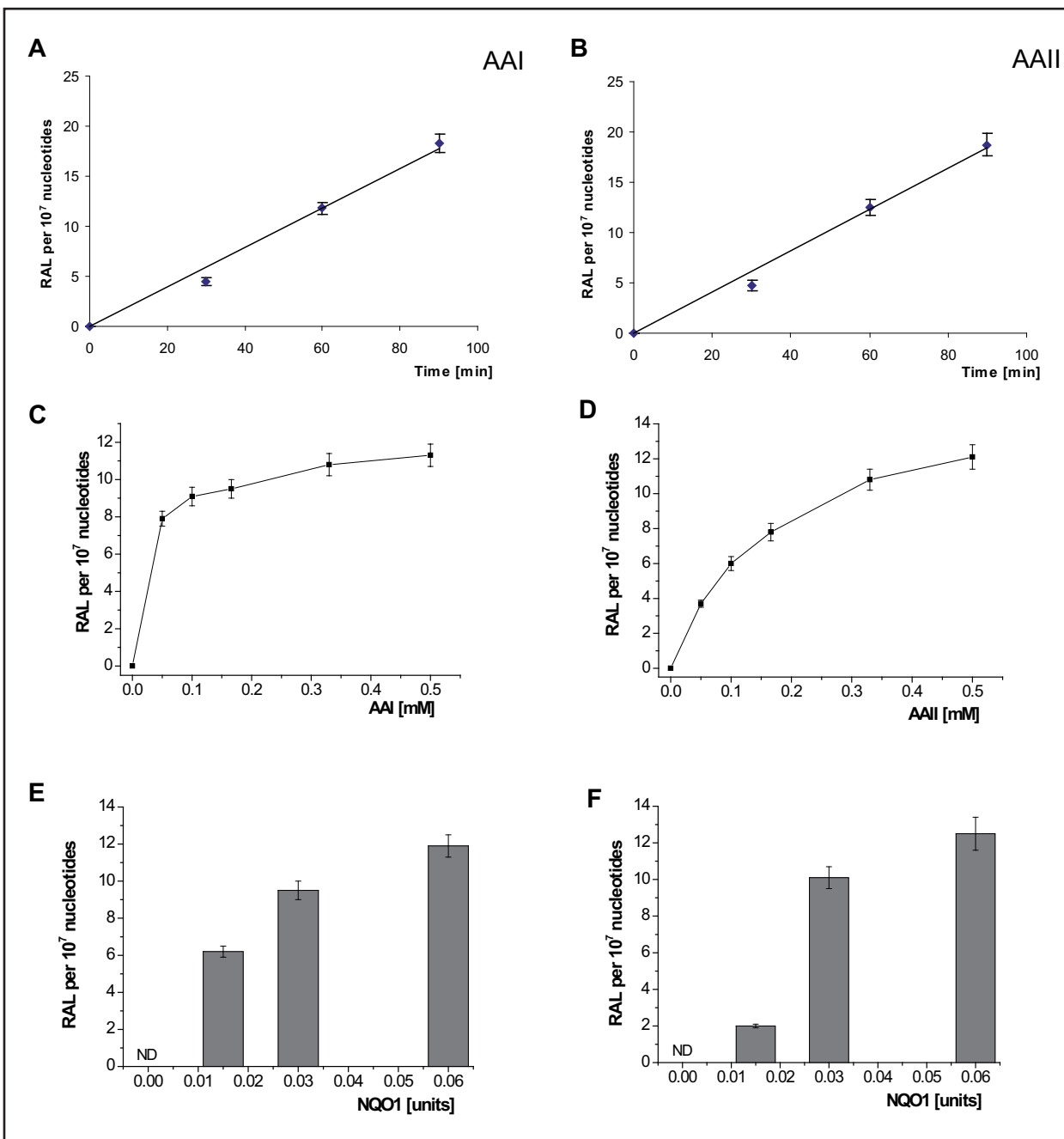


**Fig. 3.** Time-dependence of the DNA adduct formation by AAI and AAIi activated with recombinant human NQO1 (**A** and **B**). Dependence of the DNA adduct formation by AAI and AAIi activated with recombinant human NQO1 on concentrations of AAI (**C**) and AAIi (**D**) and NQO1 concentrations (**E** and **F**). Results are presented as means  $\pm$  standard deviations of triplicate *in vitro* incubations. RAL, relative adduct labeling. Data in (**A**, **C**, **E**) are taken from Stiborova *et al.* (2011).

#### Molecular docking of AAI, AAIi, their nitroso-metabolites and N-hydroxyaristolactams to the active site of NQO1

In order to examine whether the differences in the reductive activation of AAI and AAIi by NQO1 might be caused by the different potential of NQO1 to reduce these compounds, their binding to the active centre of NQO1 was modeled. Reductive activation of AAI and AAIi by NQO1 proceeds through the nitroso-derivatives and *N*-hydroxyaristolactams to form cyclic

*N*-acylnitrenium ions as the ultimate carcinogenic species binding to DNA (Figure 1). Although the molecular mechanism of the reductive activation of AAI by human NQO1 has already been partially explained (Stiborova *et al.* 2011), here we expanded our investigation to better explain also the NQO1-mediated reductive activation of AAIi. The binding of AAIi, its nitroso-derivative and aristolactam II to the active centre of human NQO1 was modeled and compared with the binding of AAI and its reductive intermediates

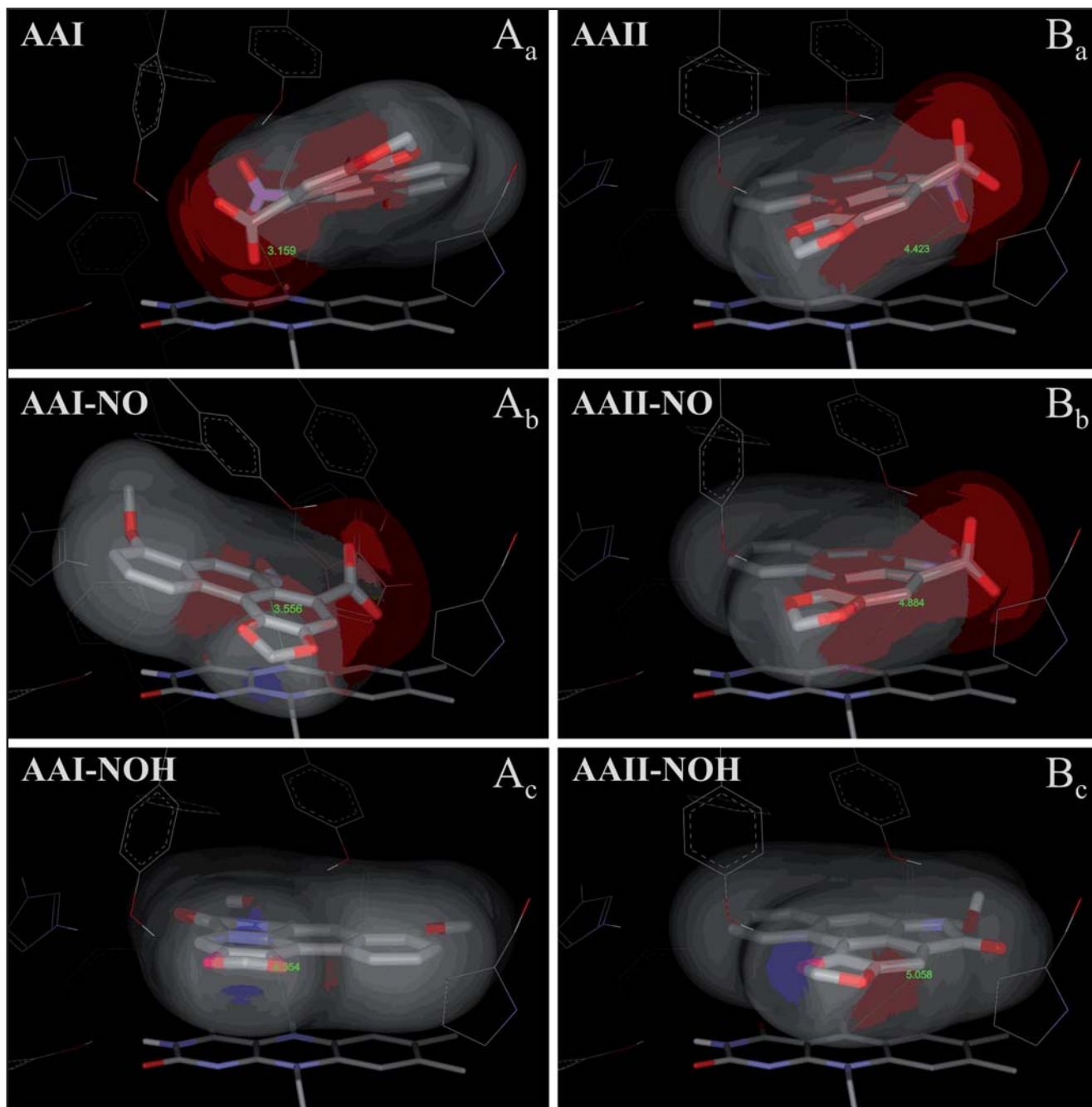


**Fig. 4.** The predicted binding orientations facilitating the hydride transfer from human NQO1 (N5 of isoalloxazine ring) to the oxygen of AAI/II (A<sub>a</sub>, B<sub>a</sub>), AAI/II nitroso-derivatives (AAI/II-NO) (A<sub>b</sub>, B<sub>b</sub>) and AAI/II *N*-hydroxylactams (AAI/I-NOH) (A<sub>c</sub>, B<sub>c</sub>). Isoalloxazine ring of reduced FAD cofactor is modelled as deprotonated anionic form. AAs or their derivatives, FAD cofactor and amino acids residues within 5.5 Å from ligand are rendered as bold sticks, and sticks and lines, respectively. Computation methods are described in Materials and Methods. Data in (A<sub>a</sub>, A<sub>b</sub>) shown for comparison are from Stiborova *et al.* (2011).

to this enzyme. *In-silico* docking of these compounds to the active site of the NQO1 dimeric molecule was performed by the soft-soft (flexible) docking procedure.

Docking calculations were performed with the natural dimeric molecule of NQO1, containing one flavin prosthetic group (FAD) per polypeptide chain. The reduced enzyme contains either of the two possible forms of reduced FAD, the anionic form (FADH<sup>-</sup>) or the protonated enol form (enol-FADH<sub>2</sub>). The calculated model structures for the complexes of NQO1 with

AAI, AAI and their reductive derivatives (nitroso-derivatives and aristolactams) (Figure 4) indicated that all these compounds bind into the active site of NQO1 with similar binding affinities. The docking calculations predicted small differences between binding affinities of AAI, AAI and their reductive derivatives toward FADH<sup>-</sup> or enol-FADH<sub>2</sub> form of NQO1. The estimated free energies of binding to NQO1 with the anionic form of FAD or the protonated enol form are shown in Table 1.

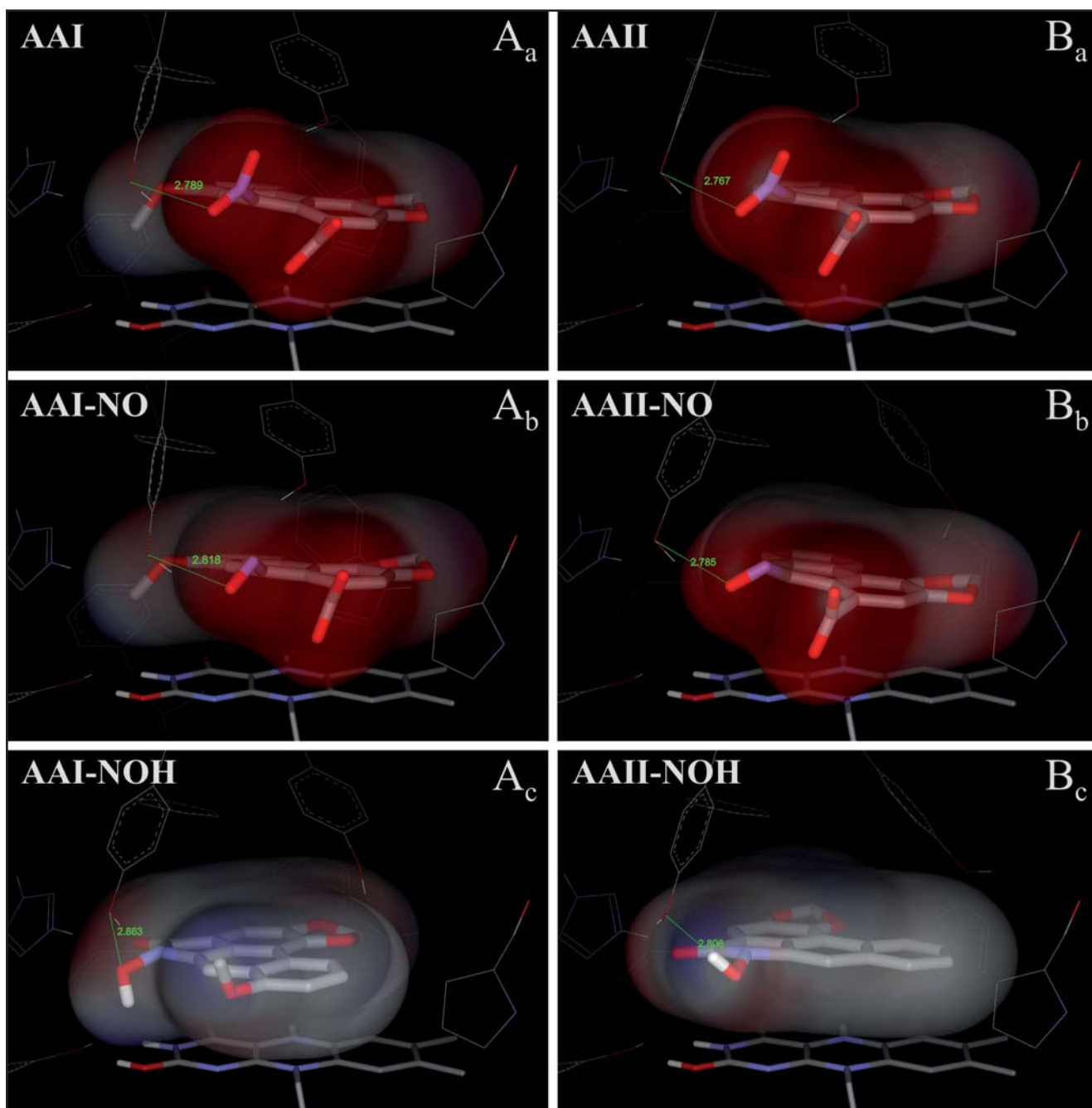


**Fig. 5.** The predicted binding orientations facilitating the alternative three-step ( $e^-$ ,  $H^+$ ,  $e^-$ ) electron transfer from NQO1 (protonated enol-form of reduced FAD) to the oxygen of AAI/II ( $A_a$ ,  $B_a$ ), AAI/II nitroso-derivatives ( $A_b$ ,  $B_b$ ) and AAI/II *N*-hydroxylactams ( $A_c$ ,  $B_c$ ). Isoalloxazine ring of reduced FAD cofactor is modelled as enolform (protonated on O2). AAs or their derivatives, FAD cofactor and amino acids residues within 5.5 Å from ligand are rendered as bold sticks, and sticks and lines, respectively. Computation methods are described in Materials and Methods. Data in ( $A_a$ ,  $B_a$ ) shown for comparison are from Stiborova *et al.* (2011).

The binding affinities of AAI and its nitroso-derivative (AAI-NO) to FADH<sup>-</sup> form of NQO1 are, however, lower by 0.5–0.6 kcal/mol in comparison to the AAI and its nitroso-derivative (AAI-NO) (Table 1). Moreover, the orientations of the AAI and AAI in the active site facilitating the direct hydride transfer are rather different (Figure 4), resulting in a greater distance of the nitro group of AAI to the hydrogen N5 of the isoalloxazine ring of FAD [4.4 Å (Figure 4B<sub>a</sub>)], than that of AAI, which is located closer to hydrogens

of this part of the FAD molecule [3.2 Å (Figure 4A<sub>a</sub>)]. Likewise, the 0.5 Å greater distances of the nitroso- and *N*-hydroxylactamoyl-groups to the hydrogen on N5 of the isoalloxazine ring of FAD were found for reductive intermediates of AAI than for those of AAI (Table 1, Figure 4). These spatial arrangements are less appropriate for a direct hydride transfer to the nitro-, nitroso- or *N*-hydroxylactamoyl-groups of AAI and its reductive intermediates in comparison to these groups of AAI and its derivatives. This finding indicates a lower effi-

ciency of NQO1 to reduce AAI to form *N*-hydroxyaristolactam II, the immediate precursor of a cyclic *N*-acylnitrenium ion that is responsible for formation of AAI-DNA adducts, resulting in slower activation of AAI. But on the other hand, decreased efficiency of NQO1 to reduce AAI-derived *N*-hydroxylactam also results in slower detoxification of AAI to aristolactam II.

However, there are still insufficient mechanistic and kinetic studies on the mechanism of substrate reduction catalyzed by NQO1. Besides a two-electron reduction mechanism by a direct hydride transfer from

N5 of a flavin cofactor to the substrate of NQO1 (Figure 4), another mechanism that can play a role in reduction of AAI was found in our former study (Stiborova *et al.* 2011). Therefore, we here investigated whether this mechanism can also contribute to NQO1-mediated reduction of AAI. In addition, the possibility of this alternative mechanism for all steps of AAI or AAI reduction (reduction of nitro-, nitroso- and *N*-hydroxylactamoyl-groups of AAs and their reductive derivatives) was evaluated (see Figure 5). For further details on proposed alternative reduction mechanism, mediated by residues Tyr128, His161 and Tyr155, see Figure 5 in Stiborova *et al.* 2011.

The predicted binding affinities of the complexes of AAI or AAI and their nitroso-derivatives with NQO1 shown in Figure 4 were 1.5–2.4 kcal/mol weaker than those of another binding mode, which facilitates the alternative three-step ( $e^-$ ,  $H^+$ ,  $e^-$ ) reduction mechanism (Figure 5, Table 1). The major factor making the direct hydride transfer more disadvantageous is probably the necessity of placing the nitro- or nitroso-group close to N5 of FAD, which results in burying the neighboring carboxylic group deep into the hydrophobic binding pocket of NQO1. Moving of this highly polar group from solution into the hydrophobic environment of the non-polar binding pocket could therefore be a significant factor destabilizing the direct hydride transfer complex. In the alternative three-step ( $e^-$ ,  $H^+$ ,  $e^-$ ) reduction complex, shown in Figure 5, however, both two AAs and their nitroso-derivatives accommodates their carboxylic group near the access channel, thereby maximizing its contact with solvent. We believe this might be the major reason why the three-step ( $e^-$ ,  $H^+$ ,  $e^-$ ) reduction mechanism can play a role in reductive activation of AAI, AAI and their nitroso-derivatives by NQO1. If we consider the mediated H-transfer mechanism the differences in binding affinities of AAI and its derivatives *vs.* AAI and its derivatives are again favoring the activation of AAI by 0.3–0.4 kcal/

**Tab. 2.** The effects of cofactors on the DNA adduct formation by AAI (A) and AAI (B) in human hepatic and renal cytosols. (A)

Human cytosolic sample	RAL <sup>a</sup> (mean ± SEM/10 <sup>8</sup> nucleotides)			
	dG-AAI	dA-AAI	dA-AAII	Total
<b>hepatic cytosol (H806)</b>				
with NADPH	5.3 ± 0.3	8.3 ± 0.4	1.0 ± 0.05	14.6 ± 0.7
NADPH+1 mM acetyl-CoA	5.4 ± 0.3	8.6 ± 0.4	1.0 ± 0.05	15.0 ± 0.7
NADPH+2 mM acetyl-CoA	3.4 ± 0.2	5.4 ± 0.3	0.6 ± 0.05	9.4 ± 0.5*
<b>hepatic cytosol (H856)</b>				
with NADPH	5.9 ± 0.2	8.0 ± 0.5	0.9 ± 0.05	14.8 ± 0.6
NADPH+0.2 mM PAPS	5.5 ± 0.3	7.6 ± 0.4	0.9 ± 0.05	14.0 ± 0.7
NADPH+0.4 mM PAPS	4.9 ± 0.2	6.6 ± 0.3	0.7 ± 0.04	12.2 ± 0.6
<b>renal cytosol</b>				
with NADPH	1.3 ± 0.05	1.5 ± 0.05	0.4 ± 0.05	3.2 ± 0.2
NADPH+2 mM acetyl-CoA	1.2 ± 0.06	1.6 ± 0.07	0.4 ± 0.05	3.2 ± 0.2
NADPH+0.4 mM PAPS	1.3 ± 0.05	1.4 ± 0.05	0.4 ± 0.05	3.1 ± 0.2

(B)

Human cytosolic sample	RAL <sup>a</sup> (mean ± SEM/10 <sup>8</sup> nucleotides)		
	dG-AAII	dA-AAII	Total
<b>hepatic cytosol (H806)</b>			
with NADPH	1.2 ± 0.1	4.6 ± 0.4	5.8 ± 0.7
NADPH+1 mM acetyl-CoA	0.5 ± 0.03	2.1 ± 0.2	2.6 ± 0.2*
NADPH+2 mM acetyl-CoA	0.1 ± 0.04	1.4 ± 0.1	1.5 ± 0.1*
<b>hepatic cytosol (H856)</b>			
with NADPH	1.3 ± 0.1	4.7 ± 0.4	6.0 ± 0.6
NADPH+0.2 mM PAPS	0.4 ± 0.03	2.0 ± 0.2	2.4 ± 0.2*
NADPH+0.4 mM PAPS	0.1 ± 0.02	1.2 ± 0.1	1.3 ± 0.1*
<b>renal cytosol</b>			
with NADPH	0.1 ± 0.01	1.6 ± 0.1	1.7 ± 0.2
NADPH+2 mM acetyl-CoA	0.03 ± 0.01	0.4 ± 0.03	0.43 ± 0.04*
NADPH+0.4 mM PAPS	0.02 ± 0.01	0.4 ± 0.02	0.42 ± 0.04*

Values are averages ± SD (n = 4) of duplicate *in vitro* incubations, each DNA sample was determined by two postlabeled analyses; 0.5 mM AAI and AAI were used. Values significantly different from control incubations without cofactors of phase II enzymes; \**p* < 0.001 (Student's *t*-test). <sup>a</sup>Relative adduct labeling. PAPS, 3'-phosphoadenosine-5'-phosphosulfate. Data in (A) are taken from Stiborova *et al.* (2011).

mol (Table 1), while the binding modes and distances of all complexes are practically identical.

*N*-hydroxylactamoyl-derivatives of AAI and AAI bind to the NQO1 in orientations allowing a direct hydride transfer to the *N*-hydroxylactamoyl group of these derivatives (Figure 4). These binding modes show similar binding affinities as their precursors, but with distances longer by ~1 Å (Table 1). In analogy to AAI or AAI, the binding orientation of the *N*-hydroxylactamoyl derivatives in the active site of NQO1 suggests that the hydride transfer to these compounds might also be indirect. However, the preference for this alternative orientation is weaker as these complexes elicit only 0.6–0.8 kcal/mol higher binding affinities than the orientations allowing the direct H-transfer (Table 1). Major loss of preference for alternative orientations of *N*-hydroxylactamoyl-derivatives can be attributed to the absence of the charged carboxylic group and an easier transfer of *N*-hydroxy group into the hydrophobic environment of the non-polar binding of NQO1.

The theoretical calculations presented in this part of our study propose that decreased binding affinities of AAI and its nitroso-derivative and/or less appropriate binding orientations of AAI and its metabolites again cause a lower efficacy of NQO1 to reduce AAI in comparison to AAI.

#### The effect of *SULT* and *NAT* cofactors on AAI- and AAI-DNA adduct formation in human hepatic and renal cytosols

In order to investigate whether the phase II enzymes *SULT*s or *NAT*s can further activate AAI and AAI, we examined the effect of cofactors on these phase II enzymes added to incubations of human cytosolic samples. For these experiments we used two human hepatic samples, one exhibiting high catalytic activity of *NAT*s, 180 nmol/min/mg protein (substrate *p*-aminosalicylic acid) and 40 nmol/min/mg protein (substrate sulfamethazine) for *NAT*1 and *NAT*2, respectively (sample H856), and the second sample that exhibits high catalytic activity of *SULT*s, 640 nmol/min/mg protein (substrate 7-hydroxycoumarin, sample H856). One human renal sample, known to be capable of activating AAI to DNA-binding species (Stiborova *et al.* 2003; 2011), was also used. The profiles of AAI- or AAI-DNA adducts formed by human hepatic and renal cytosols, consisting of the same four adducts as found in experiments investigating activation of both AAs with human NQO1 (dA-AAI, dA-AAI, dG-AAI and dG-AAI adducts, compare Figure 2), were the same with or without adding acetyl-CoA (*NAT* cofactor) or 3'-phosphoadenosine-5'-phosphosulfate (*SULT* cofactor). However, up to 2.8-fold lower levels of DNA adducts formed by AAI than by AAI were found in these cytosols. Moreover, the addition of acetyl-CoA or 3'-phosphoadenosine-5'-phosphosulfate the the incubation mixtures lead to up to ~80% inhibition of DNA adduct formation by AAI in hepatic and renal cytosols relative to incubations without both two cofac-

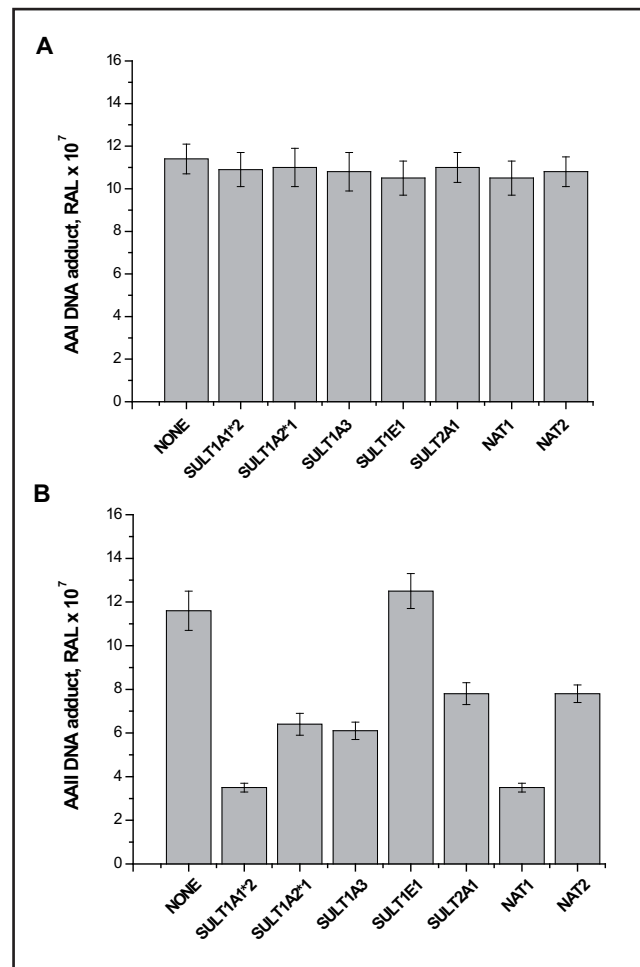


**Fig. 6.** DNA adduct formation of AAI (A) and AAI (B) (0.5 mM) after activation with human recombinant NQO1 (0.06 units) and different human recombinant *SULT*s and *NAT*s (50 µg) in presence of appropriate cofactors (0.4 mM 3'-phosphoadenosine-5'-phosphosulfate and 2 mM acetyl-CoA). Results are presented as means ± standard deviations of triplicate *in-vitro* incubations. Values significantly different from control incubations without phase II enzymes; \*\*\**p*<0.001 (Student's *t*-test). RAL, relative adduct labeling.

tors (Table 2). In contrast, only inhibition of AAI-DNA adduct formation by 2 mM acetyl-CoA was found in liver cytosol, whereas addition of this cofactor of *NAT*s at 1 mM concentration or addition of 3'-phosphoadenosine-5'-phosphosulfate to cytosolic incubations of AAI with DNA did not influence AAI-DNA adduct formation (compare Stiborova *et al.* 2011 and Table 2).

#### Metabolic activation of AAI and AAI by recombinant human *SULT*s and *NAT*s

In order to study the role of individual *SULT* and *NAT* isoenzymes in the bioactivation of AAI and AAI we used human recombinant NQO1 in combination with cytosolic extracts of baculovirus-transfected insect cells expressing human recombinant *SULT*s (*i.e.* *SULT*1A1, 1A2, 1A3, 1E, or 2A1) or *NAT*s (*i.e.* *NAT*1 or *NAT*2) in additional experiments. As shown in Figure 6, strong

DNA binding of activated AAI or AAI (0.5 mM) was observed in all incubations. The DNA adduct patterns were the same as those found in human hepatic or renal cytosols (see Figure 2). Using 50 µg of human recombinant SULTs and NATs none of these phase II enzymes stimulated DNA adduct formation by AAI or AAI (Figure 6), indicating that the slowest (rate limiting) step in metabolic activation of AAI or AAI to form DNA adducts is not the conjugation reaction. On the contrary, SULT1A1, 1A2 and 1A3 as well as NAT1 and 2 even inhibited formation of AAI-DNA adducts, by up to ~70% (Figure 6B). The SULT1A1, SULT1A2, NAT1 and NAT2 enzymes used in these experiments were capable of increasing DNA adduct levels of another aromatic nitro compound, 3-nitrobenzanthrone used as positive control, over the levels obtained with NQO1 (Arlt *et al.* 2005; Stiborova *et al.* 2010a).

## DISCUSSION

Previously we have found that AAI is, in the presence of NADPH, a cofactor of NQO1, activated by cytosolic fractions of human liver and kidney to DNA adducts identical to those found in humans suffering from Balkan endemic and aristolochic acid nephropathies (Stiborova *et al.* 2003; 2011) and concluded that NQO1 is the principle enzyme responsible for AAI activation in humans. In the present study, we demonstrate that the same cytosolic fractions were in the presence of NADPH also capable of activating AAI and show that NQO1 also plays an important role in activation of AAI. Using human recombinant NQO1, its important role in the metabolic activation of AAI and AAI to DNA-binding species was fully corroborated. Furthermore, utilizing *in silico* docking employing the soft-soft (flexible) docking procedure, here we shed more light on mechanisms of NQO1-mediated reduction of both compounds.

Using molecular modeling we found that the AAI or AAI molecules bind to the active site of human NQO1 with similar affinities, indicating that the binding orientation allows for the direct hydride transfer (*i.e.* two electron reduction) to the nitro group of both AAs. In addition, the alternative three-step ( $e^-$ ,  $H^+$ ,  $e^-$ ) two electron reduction mechanism of reduction of AAs is proposed to be more likely, as it involves more favourable binding energies. The determination of the reaction kinetics for the formation of the nitroso-derivative from AAI or AAI followed by that of *N*-hydroxyaristolactam I or II should help elucidate whether the direct hydride transfer or the proposed three step reduction occurs. This alternative two electron reduction mechanism might be relevant for the polar parts of the substrate or substrates containing charged groups (like  $COO^-$  in AAI and AAI), because the energetically unfavorable desolvation of the polar part of substrates, during their binding into the hydrophobic pocket of NQO1, would be avoided.

However, levels of AAI-DNA adducts generated in human hepatic and renal cytosols were up to 2.8-fold lower than the levels of DNA adducts formed by AAI. These results are in concordance with data published previously showing that lower levels of AAI-DNA adducts relative to AAI-DNA adducts were formed in several *in vitro* systems activating both AAs as well as *in vivo*, in rats exposed to these compounds (Schmeiser *et al.* 1988; Pfau *et al.* 1990; Stiborova *et al.* 1994; 2001a; 2001b; 2001c, 2002; 2003; 2005a; 2005b). Here we have found that one of the reasons responsible for this finding is the fact that AAI is not as good a substrate of NQO1. Indeed, although both AAI and AAI interact with the NQO1 protein and are bound with similar binding affinities to the NQO1 active site, the binding orientation of AAI in the active site of NQO1 does not favor the effective reduction of its nitro group. This result is in line with the finding that the AAI concentration required for half-maximum DNA binding (158 µM) was higher than the concentration of AAI required for DNA binding (17 µM).

The lower levels of AAI-DNA adducts found in *in vitro* experiments and *in vivo* can be also caused by the different effects of the phase II reactions on activation of AAI and AAI. Namely, in contrast to AAI-DNA adduct formation catalyzed by NQO1 that was not influenced by any of the human recombinant NAT and SULT enzymes tested in this study, the NQO1-mediated AAI-DNA adduct formation was inhibited by conjugation catalyzed with SULT1A1, 1A2 and 1A3 as well as NAT1 and NAT2. Likewise, cofactors of NAT and SULT enzymes, acetyl-CoA and 3'-phosphoadenosine-5'-phosphosulfate, respectively, strongly inhibited the DNA adduct formation by AAI in human cytosolic samples rich in these enzymes, down to 20%. This inhibition effect can also explain the finding that lower levels of AAI-DNA adducts are generated in human hepatic and renal cytosols *in vitro* even without addition of 3'-phosphoadenosine-5'-phosphosulfate or acetyl-CoA. Namely, both these cofactors and SULT and NAT enzymes are present in this subcellular systems (Stiborova *et al.* 2003; 2010a; 2011), thereby decreasing levels of AAI-DNA adducts.

All these findings indicate that NAT and SULT enzymes do not facilitate (stimulate) the bioactivation of AAI and AAI in human liver and kidney. This is unusual for nitro-aromatic compounds; conjugation reactions catalyzed by phase II enzymes are often important in the metabolic activation of such compounds (for review see Glatt 2000; Glatt *et al.* 2001; Hein 2002; Hein *et al.* 2000). Indeed, activation of 3-nitrobenzanthrone, which was used as positive control in the same experimental approach, was increased substantially by NATs and SULTs, as estimated by DNA adduct levels (Arlt *et al.* 2005; Stiborova *et al.* 2010a). Activation of AAI or AAI to species forming AAI- or AAI-DNA adducts can proceed by simple nitroreduction only, without participation of phase II enzymes

such as NATs or SULTs. While *N*-hydroxylamines (i.e. derivative of 3-nitrobenzanthrone) are relatively stable under physiological conditions and require enzymatic conjugation to be efficiently decomposed to nitrenium ions (Stiborova *et al.* 2010a), the *N*-hydroxyaristolactams under the same conditions decomposes spontaneously. Therefore, activation of AAI or AAI to species forming AAI- or AAI-DNA adducts, respectively, can proceed by simple nitroreduction, followed by spontaneous solvolysis (dissociation) producing aristolactam-oxynitrenium ions (see Figure 1), without participation of phase II enzymes such as NATs or SULTs.

Interestingly, Meinel *et al.* (2006) demonstrated that expression of human SULTs (mainly SULT1A1) in bacterial and mammalian cells reinforces the mutagenic activity of a natural mixture of AAI and AAI to these cells. However, the mechanism of this phenomenon awaits further investigations. It would be interesting to see if AAI- or AAI-DNA adduct formation in these cellular systems is modulated by the overexpression of SULT1A1.

Taking into account the results found in this study, we propose that the lower levels of DNA binding of AAI compared to AAI found *in vivo* and *in vitro* might be caused both by the lower efficiency of NQO1 to reduce this compound relative to AAI and by the inhibition effects of phase II reactions on AAI-DNA adduct formation.

## ACKNOWLEDGEMENTS

The authors would like to thank to Grant Agency of Czech Republic (grant 301/09/0472 and 203/09/0812) and to the Ministry of Education of Czech Republic (grants MSM0021620808 and 1M0505). The access to the MetaCentrum computing facilities provided under the programme LM2010005 funded by the Ministry of Education of the Czech Republic is highly appreciated.

## REFERENCES

- Arlt VM (2005) 3-Nitrobenzanthrone, a potential human cancer hazard in diesel exhaust and urban air pollution: a review of the evidence. *Mutagenesis* **20**: 399–410.
- Arlt VM, Ferluga D, Stiborova M, Pfohl-Leskowicz A, Vukelic M, Ceovic S, *et al.* (2002a) Is aristolochic acid a risk factor for Balkan endemic nephropathy-associated urothelial cancer? *Int J Cancer* **101**: 500–502.
- Arlt VM, Stiborova M and Schmeiser HH (2002b) Aristolochic acid as a probable human cancer hazard in herbal remedies: a review. *Mutagenesis* **17**: 265–277.
- Arlt VM, Stiborova M, vom Brocke J, Simoes ML, Lord GM, Nortier JL, *et al.* (2007) Aristolochic acid mutagenesis: molecular clues to the aetiology of Balkan endemic nephropathy-associated urothelial cancer. *Carcinogenesis* **28**: 2253–2261.
- Arlt VM, Stiborova M, Henderson CJ, Osborne MR, Bieler CA, Frei E, *et al.* (2005) Environmental pollutant and potent mutagen 3-nitrobenzanthrone forms DNA adducts after reduction by NAD(P)H: quinone oxidoreductase and conjugation by acetyltransferases and sulfotransferases in human hepatic cytosols. *Cancer Res* **65**: 2644–2652.
- Arlt VM, Zuo J, Trenz K, Roufosse CA, Lord GM, Nortier JL, *et al.* (2011) Gene expression changes induced by the human carcinogen aristolochic acid I in renal and hepatic tissue of mice. *Int J Cancer* **128**: 21–32.
- Bieler CA, Stiborova M, Wiessler M, Cosyns JP, van Ypersele de Strihou C and Schmeiser HH (1997) <sup>32</sup>P-post-labelling analysis of DNA adducts formed by aristolochic acid in tissues from patients with Chinese herbs nephropathy. *Carcinogenesis* **18**: 1063–1067.
- Cavelier G and Amzel LM (2001) Mechanism of NAD(P)H: quinone reductase: Ab initio studies of reduced flavin. *Proteins* **43**: 420–432.
- Chan W, Luo HB, Zheng Y, Cheng YK and Cai Z (2007) Investigation of the metabolism and reductive activation of carcinogenic aristolochic acids in rats. *Drug Metab Dispos* **35**: 866–874.
- Cleland WW (1983) Statistical analysis of the enzyme kinetic data. *Methods Enzymol* **63**: 103–138.
- Debelle FD, Vanherweghem JL and Nortier JL (2008) Aristolochic acid nephropathy: a worldwide problem. *Kidney Int* **74**: 158–169.
- Faig M, Bianchet MA, Talalay P, Chen S, Winski S, Ross D, *et al.* (2000) Structures of recombinant human and mouse NAD(P)H: quinone oxidoreductases: species comparison and structural changes with substrate binding and release. *Proc Natl Acad Sci USA* **97**: 3177–3182.
- Faig M, Bianchet MA, Winski S, Hargreaves R, Moody CJ, Hudnott AR, *et al.* (2001) Structure-based development of anticancer drugs: complexes of NAD(P)H: quinone oxidoreductase 1 with chemotherapeutic quinines. *Structure* **9**: 659–667.
- Frisch MJ, Trucks GW, Schlegel HB, Scuseria GE, Robb MA, Cheeseman JR, *et al.* (2003) Gaussian 03, Gaussian, Inc., Wallingford, CT.
- Glatt H (2000) Sulfotransferases in the bioactivation of xenobiotics. *Chem Biol Interact* **129**: 141–170.
- Glatt H, Boeing H, Engelke CEH, Kuhlow LMA, Pabel U, Pomplun D, *et al.* (2001) Human cytosolic sulphotransferases: genetics, characteristics, toxicological aspects. *Mutat Res* **482**: 27–40.
- Grollman AP, Shibutani S, Moriya M, Miller F, Wu L, Moll U, *et al.* (2007) Aristolochic acid and the etiology of endemic (Balkan) nephropathy. *Proc Natl Acad Sci USA* **104**: 12129–12134.
- Grosse Y, Baan R, Straif K, Secretan B, El Ghissassi F, Bouvard V, *et al.* (2009) A review of human carcinogens-Part A: pharmaceuticals. *Lancet Oncol* **10**: 13–14.
- Hein DW (2002) Molecular genetics and function of NAT1 and NAT2: role in aromatic amine metabolism and carcinogenesis. *Mutat Res* **506–507**: 65–77.
- Hein DW, Doll MA, Fretland AJ, Leff MA, Webb SJ, Xiao GH, *et al.* (2000) Molecular genetics and epidemiology of the NAT1 and NAT2 acetylation polymorphisms. *Cancer Epidemiol Biomarkers Prev* **9**: 29–42.
- Huey R, Morris G M, Olson AJ and Goodsell DS (2007) A semiempirical free energy force field with charge-based desolvation. *J Comput Chem* **28**: 1145–1152.
- Kohara A, Suzuki T, Honma M, Ohwada T and Hayashi M (2002) Mutagenicity of aristolochic acid in the lambda/lacZ transgenic mouse (MutaMouse). *Mutat Res* **515**: 63–72.
- Lai MN, Wang SM, Chen PC, Chen YY and Wang JD (2010) Population-based case-control study of Chinese herbal products containing aristolochic acid and urinary tract cancer risk. *J Natl Cancer Inst* **102**: 179–186.
- Lemy A, Wissing KM, Rorive S, Zlotta A, Roumeguere T, Muniz Martinez MC, *et al.* (2008) Late onset of bladder urothelial carcinoma after kidney transplantation for end-stage aristolochic acid nephropathy: a case series with 15-year follow-up. *Am J Kidney Dis* **51**: 471–477.
- Li R, Bianchet MA, Talalay P and Amzel LM (1995) The three-dimensional structure of NAD(P)H: quinone reductase, a flavoprotein involved in cancer chemoprotection and chemotherapy: Mechanism of the two-electron reduction. *Proc Natl Acad Sci USA* **92**: 8846–8850.
- Lord GM, Cook T, Arlt VM, Schmeiser HH, Williams G and Pusey CD (2001) Urothelial malignant disease and Chinese herbal nephropathy. *Lancet* **358**: 1515–1516.

- 27 Lord GM, Hollstein M, Arlt VM, Roufousse C, Pusey CD, Cook T *et al.* (2004) DNA adducts and p53 mutations in a patient with aristolochic acid-associated nephropathy. *Am J Kidney Dis* **43**: e11–17.
- 28 Mei N, Arlt VM, Phillips DH, Heflich RH and Chen T (2006) DNA adduct formation and mutation induction by aristolochic acid in rat kidney and liver. *Mutat Res* **602**: 83–91.
- 29 Meinel W, Pabel U, Osterloh-Quitroz H, Hengstler JG and Glatt H (2006) Human sulphotransferases are involved in the activation of aristolochic acids and are expressed in renal target tissue. *Int J Cancer* **118**: 1090–1097.
- 30 Nedelko T, Arlt VM, Phillips DH and Hollstein M (2009) TP53 mutation signature supports involvement of aristolochic acid in the aetiology of endemic nephropathy-associated tumours. *Int J Cancer* **124**: 987–990.
- 31 Nortier JL, Martinez MC, Schmeiser HH, Arlt VM, Bieler CA, Petein M, *et al.* (2000) Urothelial carcinoma associated with the use of a Chinese herb (*Aristolochia fangchi*). *N Engl J Med* **342**: 1686–1692.
- 32 Pfau W, Schmeiser HH and Wiessler M (1990) <sup>32</sup>P-postlabelling analysis of the DNA adducts formed by aristolochic acid I and II. *Carcinogenesis* **11**: 1627–1633.
- 33 Phillips DH and Arlt VM (2007) The <sup>32</sup>P-postlabeling assay for DNA adducts. *Nature Prot* **2**: 2772–2781.
- 34 Ross D, Kepa JK, Winski SL, Beall HD, Anwar A and Siegel D (2000) NAD(P)H: quinone oxidoreductase (NQO1): chemoprotection, bioactivation, gene regulation and genetic polymorphisms. *Chem-Biol Interact* **129**: 77–97.
- 35 Schmeiser HH, Bieler CA, Wiessler M, van Ypersele de Strihou C and Cosyns JP (1996) Detection of DNA adducts formed by aristolochic acid in renal tissue from patients with Chinese herbs nephropathy. *Cancer Res* **56**: 2025–2028.
- 36 Schmeiser HH, Frei E, Wiessler M and Stiborova M (1997) Comparison of DNA adduct formation by aristolochic acids in various in vitro activation systems by <sup>32</sup>P-postlabelling: evidence for reductive activation by peroxidase. *Carcinogenesis* **18**: 1055–1062.
- 37 Schmeiser HH, Pool BL and Wiessler M (1984) Mutagenicity of the two main components of commercially available carcinogenic aristolochic acid in *Salmonella typhimurium*. *Cancer Lett* **23**: 97–101.
- 38 Schmeiser HH, Schoepe K-B, and Wiessler M (1988) DNA adduct formation of aristolochic acid I and II in vitro and in vivo. *Carcinogenesis* **9**: 297–303.
- 39 Schmeiser HH, Stiborova M and Arlt VM (2009) Chemical and molecular basis of the carcinogenicity of *Aristolochia* plants. *Curr Opin Drug Discov Devel* **12**: 141–148.
- 40 Shibutani S, Dong H, Suzuki N, Ueda S, Miller F and Grollman AP (2007) Selective toxicity of aristolochic acids I and II. *Drug Metab Dispos* **35**: 1217–1222.
- 41 Simoes ML, Hockley SL, Schwerdtle T, da Costa GG, Schmeiser HH, Phillips DH *et al.* (2008) Gene expression profiles modulated by the human carcinogen aristolochic acid I in human cancer cells and their dependence on TP53. *Toxicol Appl Pharmac* **232**: 86–98.
- 42 Sistkova J, Hudecek J, Hodek P, Frei E, Schmeiser HH and Stiborova M (2008) Human cytochromes P450 1A1 and 1A2 participate in detoxication of carcinogenic aristolochic acid. *Neuro Endocrinol Lett* **29**: 733–737.
- 43 Smith G, Stanley LA, Sim E, Strange RC and Wolf R (1995) Metabolic polymorphism and cancer susceptibility. *Cancer Surveys* **25**: 27–65.
- 44 Stiborova M, Asfaw B and Anzenbacher P (1988) Activation of carcinogens by peroxidase. Horseradish peroxidase-mediated formation of benzenediazonium ion from a non-aminoazo dye, 1-phenylazo-2-hydroxynaphthalene (Sudan I) and its binding to DNA. *FEBS Lett* **232**: 387–390.
- 45 Stiborova M, Fernando RC, Schmeiser HH, Frei E, Pfau W and Wiessler M (1994) Characterization of DNA adducts formed by aristolochic acids in the target organ (forestomach) of rats by <sup>32</sup>P-postlabelling analysis using different chromatographic procedures. *Carcinogenesis* **15**: 1187–1192.
- 46 Stiborova M, Frei E, Arlt VM and Schmeiser HH (2008a) Metabolic activation of carcinogenic aristolochic acid, a risk factor for Balkan endemic nephropathy. *Mutat Res* **658**: 55–67.
- 47 Stiborova M, Frei E, Breuer A, Wiessler M and Schmeiser HH (2001a) Evidence for reductive activation of carcinogenic aristolochic acids by prostaglandin H synthase – <sup>32</sup>P-postlabeling analysis of DNA adduct formation. *Mutat Res* **493**: 149–160.
- 48 Stiborova M, Frei E, Hodek P, Wiessler M and Schmeiser HH (2005a) Human hepatic and renal microsomes, cytochromes P450 1A1/2, NADPH: cytochrome P450 reductase and prostaglandin H synthase mediate the formation of aristolochic acid-DNA adducts found in patients with urothelial cancer. *Int J Cancer* **113**: 189–197.
- 49 Stiborova M, Frei E and Schmeiser HH (2008b) Biotransformation enzymes in development of renal injury and urothelial cancer caused by aristolochic acid. *Kidney Int* **73**: 1209–1211.
- 50 Stiborova M, Frei E, Sopko B, Sopkova K, Markova V, Lankova M *et al.* (2003) Human cytosolic enzymes involved in the metabolic activation of carcinogenic aristolochic acid: evidence for reductive activation by human NAD(P)H: quinone oxidoreductase. *Carcinogenesis* **24**: 1695–1703.
- 51 Stiborova M, Frei E, Sopko B, Wiessler M and Schmeiser HH (2002) Carcinogenic aristolochic acids upon activation by DT-diaphorase form adducts found in DNA of patients with Chinese herbs nephropathy. *Carcinogenesis* **23**: 617–625.
- 52 Stiborova M, Frei E, Wiessler M and Schmeiser HH (2001b) Human enzymes involved in the metabolic activation of carcinogenic aristolochic acids: evidence for reductive activation by cytochromes P450 1A1 and 1A2. *Chem Res Toxicol* **14**: 1128–1137.
- 53 Stiborova M, Hajek M, Frei E and Schmeiser HH (2001c) Carcinogenic and nephrotoxic alkaloids aristolochic acids upon activation by NADPH: cytochrome P450 reductase form adducts found in DNA of patients with Chinese herbs nephropathy. *Gen Physiol Biophys* **20**: 375–392.
- 54 Stiborova M, Hajek M, Vosmikova H, Frei E and Schmeiser HH (2001d) Isolation of DT-diaphorase [NAD(P)H dehydrogenase (quinone)] from rat liver cytosol: identification of new enzyme substrates, carcinogenic aristolochic acids. *Collect Czech Chem Commun* **66**: 959–972.
- 55 Stiborova M, Mares J, Frei E, Arlt VM, Martinek V and Schmeiser HH (2011) The human carcinogen aristolochic acid I is activated to form DNA adducts by human NAD(P)H: quinone oxidoreductase without the contribution of acetyltransferases or sulfotransferases. *Environ. Mol. Mutagen* **52**: 448–459.
- 56 Stiborova M, Martinek V, Svobodova M, Sistkova J, Dvorak Z, Ulrichova J *et al.* (2010a) Mechanisms of the different DNA adduct forming potentials of the urban air pollutants 2-nitrobenzanthrone and carcinogenic 3-nitrobenzanthrone. *Chem Res Toxicol* **23**: 1192–1201.
- 57 Stiborova M, Moserova M, Mrazova B, Kotrbova V and Frei E. (2010b) Role of cytochromes P450 and peroxidases in metabolism of the anticancer drug ellipticine: additional evidence of their contribution to ellipticine activation in rat liver, lung and kidney. *Neuro Endocrinol. Lett.* **31**(Suppl. 2): 26–35.
- 58 Stiborova M, Sopko B, Hodek P, Frei E, Schmeiser HH and Hudecek J (2005b) The binding of aristolochic acid I to the active site of human cytochromes P450 1A1 and 1A2 explains their potential to reductively activate this human carcinogen. *Cancer Lett* **229**: 193–204.
- 59 Svobodova M, Martinkova M, Dracinska H, Frei E and Stiborova M (2009) Rat cytochromes P450 oxidize 2-nitrophenol, a human metabolite of carcinogenic 2-nitroanisole. *Neuro Endocrinol Lett.* **30** (Suppl. 1): 46–51.
- 60 Vanherweghem JL, Depierreux M, Tielemans C, Abramowicz D, Dratwa M, Jadoul M *et al.* (1993) Rapidly progressive interstitial renal fibrosis in young women: association with slimming regimen including Chinese herbs. *Lancet* **341**: 387–391.